[CANCER RESEARCH 60, 2122–2127, April 15, 2000]

Advances in Brief

Metabolites of 2′-Fluoro-2′-deoxy-D-glucose Detected by ^{19}F Magnetic Resonance Spectroscopy *in Vivo* Predict Response of Murine RIF-1 Tumors to 5-Fluorouracil[1]

Paul M. J. McSheehy,[2] Martin O. Leach, Ian R. Judson, and John R. Griffiths

Cancer Research Campaign Biomedical Magnetic Resonance Research Unit, Department of Biochemistry and Immunology, St. George's Hospital Medical School, London SW17 0RE, United Kingdom [P. M. J. M., J. R. G.], and Cancer Research Campaign Clinical Magnetic Resonance Research Group [P. M. J. M., M. O. L.] and Cancer Research Campaign Centre for Cancer Therapeutics [P. M. J. M., I. R. J.], Institute of Cancer Research and Royal Marsden NHS Trust, Sutton, Surrey SM2, United Kingdom

Abstract

There is a clinical need for early detection of tumor response to therapy. This study aimed to determine whether metabolites of fluorodeoxyglucose (FDG) detected in solid mouse tumors *in situ* by ^{19}F magnetic resonance spectroscopy (^{19}F MRS) correlated with response to 5-fluorouracil chemotherapy. After injection of FDG (1.4 mmol/kg i.p.), uptake and metabolism was monitored for 2 h in RIF-1 tumors. FDG was detectable immediately, and after 10 min, a second broad peak was detected 5–6 ppm upfield. ^{19}F MRS analysis of cell and tumor extracts *in vitro* showed that the upfield peak (≥15% of the total detectable ^{19}F signal) consisted of the epimer α-fluorodeoxymannose (FDM) and various conjugates. Mice treated with 5-fluorouracil (130 mg/kg) received, 48 h later, a repeat dose of FDG. The change in the rate of FDM formation, but not the FDG or total ^{19}F signal, correlated significantly with the response to 5-fluorouracil ($P = 0.032$), suggesting that ^{19}F MRS of FDM metabolism *in vivo* may be a novel means of predicting tumor response.

Introduction

High aerobic glycolysis is part of the tumor phenotype, associated with raised rates of glucose transport and phosphorylation and decreased glucose-6-phosphate dephosphorylation (1). This phenomenon allows noninvasive detection of solid tumors in the clinic using PET[3] images obtained from distribution of the radioactive glucose analogue 2′-^{18}fluoro-2′-deoxyglucose (^{18}FDG). FDG uptake by tumors can be proportional to the number of viable cells, which may allow prediction of response after chemo- or radiotherapy. However, prediction of response is not always successful because after therapy, one or more events may occur: (*a*) the fraction of cells in S-phase may either increase or decrease; (*b*) changes in tumor blood flow may affect FDG delivery; and (*c*) the number of glycolytic macrophages that infiltrate the tumor may change (2). An additional problem is that the PET method does not distinguish FDG from FDG-6P, or indeed any additional metabolites, which could complicate the three-compartment modeling that is used to determine the rate of glycolysis. Although the PET approach assumes that FDG is only metabolized to FDG-6P (2), there is in fact abundant evidence from ^{19}F MRS that further metabolism occurs in several different types of tissues (3). Like PET, the noninvasive technique of ^{19}F MRS is also unable to resolve FDG-6P signals from FDG *in vivo*, but studies of rodent brain, heart, and ascites have shown that FDG-6P can epimerize to FDM-6P, which is readily resolved from the FDG group (FDG and FDG-6P, *i.e.*, FDG±P) *in vivo* (3–6). The FDM-6P undergoes further metabolism to nucleoside-diphosphate-FDM, very likely UDP-FDM (Fig. 1), which can persist in tissues for up to 48 h (3). If ^{19}F MRS could measure the rate of FDG-6P metabolism or a surrogate of FDG-6P in solid tumors *in vivo*, then a useful clinical tool might be available. In this study, we aimed to determine whether ^{19}F MRS could detect metabolism of FDG beyond FDG-6P in solid murine tumors *in vivo* and whether FDG uptake (total ^{19}F signal) or formation of FDM metabolites correlated with tumor response to chemotherapy.

Materials and Methods

Chemicals and Media. ^{19}FDG and 6AN were obtained from Sigma Chemical Co. (Poole, Dorset, United Kingdom). FDG was dissolved in 0.9% saline to provide a stock concentration of 137.3 mM and stored at −20°C for up to 2 months. 5FU was obtained from David Bull Laboratories (Warwick, United Kingdom) as a saline solution of 192 mM. HK, PGI, glucose-6-phosphate dehydrogenase, and NADP were obtained from Boehringer Mannheim (Lewes, East Sussex, United Kingdom). All cell culture materials were obtained from Life Technologies, Inc. (Paisley, United Kingdom). A kit for measuring cell protein based upon the Biuret method was obtained from the Sigma Chemical Co. (Poole, Dorset, United Kingdom).

Tumors and Experimental Set-Up *in Vivo*. Murine RIFs (RIF-1) were grown in C3H mice, and tumor volume was calculated as described previously (7). Anesthetized animals were placed in the bore of a Varian 200/330 4.7T spectrometer with tumors (0.4–1 g) hung into a dual-tuned ^{1}H/^{19}F surface coil (12-mm diameter) with a reference bulb containing 10 μl of 5FU (2 μmol). FDG was injected i.p. as a 0.2-ml bolus (1.4 mmol/kg), and nonlocalized ^{19}F spectra were acquired immediately in 10-min blocks for 120 min (12 × 1500 transients of 0.4 s) using a spectral width of 20 KHz with a 45° pulse at the coil center. Seven mice received a single dose of 5FU (1 mmol/kg, i.p.) 3 h after the initial FDG injection, This dose of 5FU is known to cause significant shrinkage of RIF-1 tumors within 48 h, with maximum decreases observed at 3–5 days, followed by a return to pretreatment size after ~10 days (7). After 48 h, the ^{19}F MRS experiment was repeated using a second dose of FDG. The response to 5FU was assessed by measuring tumors every 2 or 3 days for at least 7 days and recording: (*a*) the MXD; and (*b*) the TV7.

Extracts and Analyses *in Vitro*. Some RIF-1 tumors were not treated with 5FU but instead were freeze-clamped 2 h after FDG treatment for ^{19}F MRS analysis *in vitro* at 4.7 T, or in some cases using a vertical high-resolution 8.5T Bruker system. Perchlorate extracts were made as described previously (8), and 5FU was added to a final concentration of 2 mM to act as an internal standard for quantitation. Perchlorate extracts were also made from: (*a*) plasma samples of 0.25 ml obtained from mice 30 min after injection of FDG; and (*b*) cultured RIF-1 cells. Confluent RIF-1 cell cultures were incubated for 4 h with

Received 10/25/99; accepted 3/2/00.

The costs of publication of this article were defrayed in part by the payment of page charges. This article must therefore be hereby marked *advertisement* in accordance with 18 U.S.C. Section 1734 solely to indicate this fact.

[1] This work was supported by the Cancer Research Campaign (CRC) Program Grant SP1971/0503.

[2] To whom requests for reprints should be addressed, at Cancer Research Campaign Biomedical Magnetic Resonance Research Unit, Department of Biochemistry and Immunology, St. George's Hospital Medical School, Cranmer Terrace, London SW17 0RE, United Kingdom.

[3] The abbreviations used are: PET, positron emission tomography; FDG, 2′-fluoro-2′-deoxy-D-glucose; FDG-6P, FDG-6-phosphate; FDM, 2′-fluoro-2′-deoxy-D-mannose; FDM-6P, FDM-6-phosphate; FDG±P, FDG with/without phosphate; FDM±P, FDM with/without phosphate; 5FU, 5-fluorouracil; MRS, magnetic resonance spectroscopy; 6AN, 6-aminonicotinamide; RIF, radiation-induced fibrosarcoma; AUC, area under the concentration-time curve; 6PG, 6-phosphogluconate; PPP, pentose phosphate pathway; HK, hexokinase; PGI, phosphoglucoisomerase; MXD, maximum decrease in tumor volume; TV7, decrease in tumor volume at 7 days.

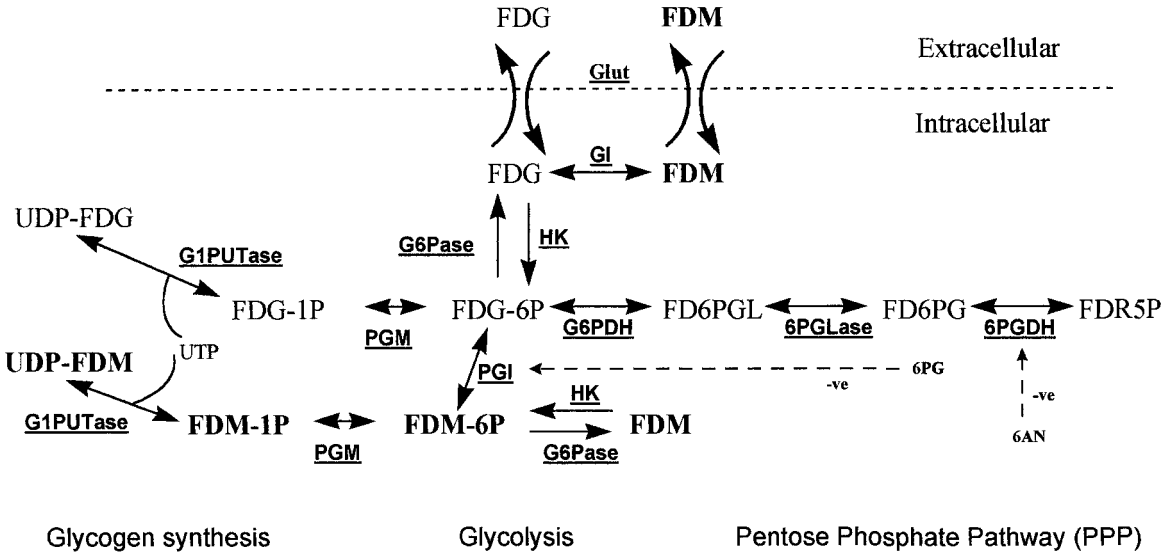

Fig. 1. Metabolism of FDG. Metabolites of FDG that may be resolved from FDG *in vivo* by ^{19}F MRS are shown in boldface. Metabolites shown are: *FDG-6P* or *FDG-1P*, 2-fluoro-2-deoxy-D-glucose-6-phosphate or 1-phosphate; *FDM-6P* or *FDM-1P*, 2-fluoro-2-deoxymannose-6-phosphate or 1-phosphate; *UDP-FDG* or *UDP-FDM*, UDP-2-fluoro-2-deoxyglucose/mannose; *FD6PGL*, 2-fluoro-2-deoxyglucose-6-phosphogluco-δ-lactone; *FD6PG*, 2-fluoro-2-deoxyglucose-6-phosphogluconates; *FDR5P*, 2-fluoro-2-deoxyribulose-5-phosphate. Enzymes are underlined. *Glut*, glucose transporter; *GI*, glucose isomerase; *HK*, hexokinase; *G6Pase*, glucose-6-phosphatase; *PGI*, phosphoglucoisomerase; *PGM*, phosphoglucomutase; *G1PUTase*, glucose-1-phosphate uridyltransferase; *G6PDH*, glucose-6-phosphate dehydrogenase; *6PGLase*, 6-phosphogluco-δ-lactonase; *6PGDH*, 6-phosphogluconate dehydrogenase.

or without 200 μM 6AN prior to the addition of 1.5 mM FDG. After 2 h, the medium was removed, the cell monolayer was washed with PBS, and the cells were detached by using a 0.01 M EDTA-trypsin mix. The cells were briefly centrifuged, and the pellet was extracted (8). Quantitative analysis of tumor or cell extracts by ^{19}F MRS was performed at 4.7 T on 1-ml samples using a spectral width of 20 KHz, a 90° pulse, and 4000 × 14.5-s transients. Spectra received 20 Hz line broadening, and peak integrals were measured by FITSPEC, as described previously (7). This method provided a sensitivity limit of 10 nmol. Extracts of isolated cells were scanned for at least 10,000 transients. ^{19}F MRS at high resolution was performed at 8.5 T on 1-ml samples using a spectral width of 24 KHz, a 22° pulse, and 10,000 × 6-s transients. Spectra received 2 Hz line broadening.

Enzyme Analyses. Confluent cultures of RIF-1 cells were trypsinized, centrifuged, and resuspended in 1 ml (>10^7 cells/ml), before the addition of Triton X-100 to a final concentration of 1%. The cell suspension was then frozen at −20°C and used for enzyme analysis within 24 h. Prior to enzymatic analysis, cell suspensions were freeze-thawed once more and maintained at 4°C. HK and PGI activity were assayed spectrophotometrically at 25°C by recording the absorbance of NADP at 340 nm, according to the methods described by Bergmeyer (9). The assay efficiency was tested by testing dilutions of the pure enzymes to check that 1 unit of enzyme activity produced 1 μmol substrate per minute. Results were expressed as milliunits/mg cell protein from duplicate samples.

Data Analysis. All ^{19}F data were analyzed as described previously to calculate the peak integrals and chemical shifts (7). Under the conditions used *in vivo*, FDG and metabolites were 32% saturated, and the 5FU external standard was 74% saturated; appropriate corrections allowed estimation of drug concentrations in the tumor. Graphical representation of the data (peak integral *versus* time) allowed calculation of the AUC for the FDG and FDM groups and total ^{19}F, as μmoles formed in 2 h per g tumor, and linear regression was used to calculate the rate of total (α- plus β-) FDM formation as nmol/min/g tumor. The strength of the relationship between parameters was measured using linear regression to obtain the correlation coefficient *r* and the associated *P* for significance (<0.05).

Results

FDG in 0.9% Saline at 4.7 T. The α- and β-anomers of FDG were readily resolved from one another in the stock solution; the two peaks showed a chemical shift (δ_F) difference of 0.25 ppm when 10 Hz line broadening was used. T_1s of 1.74 ± 0.03 and 1.85 ± 0.03 s, respectively, were measured, comparable with values measured in cells by Kojima *et al.* (4), who reported that FDG and FDM and their conjugates all had similar T_1s. Increasing the number of transients to 6400 × 9 s allowed detection of an additional peak at −6.0 ppm (upfield), consistent with the presence of a small amount of FDM (0.13 μmol/ml). This low level of FDM contamination (0.09%) in the stock solution would be undetectable *in vivo*; therefore, any FDM detected *in vivo* would have to be attributable to FDG metabolism.

^{19}F MRS of FDG in RIF-1 Tumors *in Vivo*. The FDG signal (0 ppm) appeared at −31 ppm (upfield) from the 5FU reference within 2 min after administration. In 2 of 13 tumors, the maximum signal intensity (*Cmax*) of this group (α-FDG ± 6P plus β-FDG ± 6P) developed within 10 min; in the other 11 tumors, it was after 30 min (Fig. 2). The T_1 of the FDG group measured in three different tumors *in vivo* was 1.35 ± 0.03 s (mean ± SE) at 30−60 min after injection. In all tumors studied, the major FDM group (α-FDM±P) was detectable after 10 min at −5.3 ppm from the FDG group, and sometimes, the minor FDM group (β-FDM±P) was detectable after 60 min further upfield at −23.8 ppm. The mean *Cmax* of the FDG group was 1.8 ± 0.2 mM at 60 min after injection, whereas the FDM group increased linearly up to 110 min, allowing calculation of a rate of formation of 2.3 ± 0.5 nmol/min/g (mean ± SE; $n = 10$). Unlike in brain tissue (3, 5, 6), metabolites of the PPP (approximately +3 ppm downfield from FDG) were not detectable. In some cases, a small peak corresponding to UDP-FDG could be detected at approximately −2 ppm (Fig. 2*b*). In a separate cohort of three mice, the plasma concentration was determined to be 1.6 ± 0.2 mM (mean ± SE) 30 min after injection, similar to the concentration calculated for tumor FDG *in vivo*.

High resolution analysis of tumor extracts *in vitro* by ^{19}F MRS at 8.5 T confirmed the absence of peaks downfield from the FDG group but revealed the presence of numerous other metabolites of FDG (Fig. 3). These peaks have been described in mouse brain (6), allowing the assignments described in Fig. 3 and below. On the basis of these previous assignments, the major group of peaks (fig. 3*a*) are the β- and α-anomers of FDG-6P and FDG-1P, whereas the doublet on Fig. 3*b* would be the β- and α-anomers of UDP-FDG. The next group of

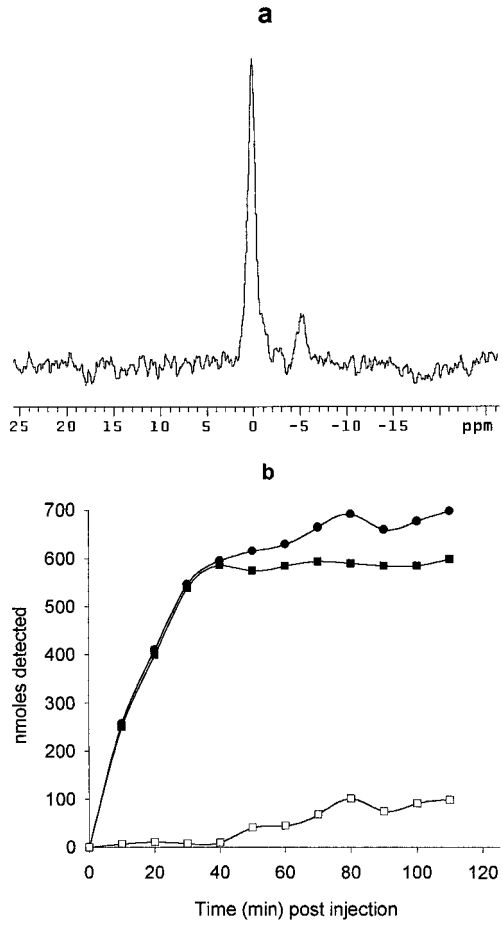

Fig. 2. Detection *in vivo* of FDG uptake and metabolism. Results are from a typical RIF-1 tumor of 0.33 g and show: *a*, the ^{19}F MRS signals detected at 100–120 min after injection: α and β-FDG group, *i.e.*, FDG±P (0 ppm), α-FDM group, *i.e.*, FDM±P (5 ppm); and *b*, the complete time course from 0–120 min. ●, total ^{19}F-signal; ■, FDG±P; □, FDM±P. Quantitative ^{19}F MRS at 4.7 T of the tumor extract showed that the amounts of FDG±P and FDM±P were 525 and 95 nmol, respectively, after 120 min.

peaks upfield at Fig. 3, *c* and *d*, is the α-FDM group, beginning with FDM-1,6-P_2 and FDM-1P (Fig. 3*c*), followed by FDM-6P, FDM, and the most upfield peak in this group, UDP-FDM (Fig. 3*d*). Fig. 3*e* is the β-FDM±P group. Peak integration showed that the combined FDM groups (Fig. 3, *c–e*) were 18–20% of the total ^{19}F signal detectable, demonstrating that considerable metabolism had occurred beyond FDG-6P at 2 h after injection.

FDG Metabolism in Cultured RIF-1 Cells. Extracts from 2×10^7 isolated cells contained 31 nmol of α-FDM±P and 204 nmol FDG±P after 2 h incubation with 1.5 mM FDG. β-FDM±P was not detectable in these cell extracts. Assuming a cell volume of 40 μl/10^7 cells (10), this would be equivalent to 0.38 mM FDM±P, similar to the concentrations formed *in vivo* after 2 h. Assuming approximately 2×10^8 RIF-1 cells/g tumor tissue and linear rates of FDM formation, this would correspond to a formation rate of 2.6 nmol/min/g, similar to the rate determined *in vivo* (see above). Higher FDG concentrations (15 mM) led to formation of ~1 mM FDM±P in 2 h. α- or β-FDM±P was not detectable in cultures incubated for 1 min with FDG or in cultures preincubated with 6AN prior to FDG. Low levels of FDG±P and UDP-FDG, 80 and 12 nmol, respectively, were however detectable in extracts obtained from cells incubated with 6AN.

Enzyme Activity of HK and PGI. The mean activity of HK was 43 ± 12 millunits/mg, which in each of four preparations was always exceeded by PGI, giving a mean activity of 2000 ± 250 milliunits/mg (mean ± SE). The mean ratio of PGI/HK activity was 64 ± 26.

Effect of 5FU Treatment on FDG Metabolism *in Vivo*. The total ^{19}F signal or FDG AUC showed very little change after 5FU treatment; the ratios before and after treatment were 1.04 ± 0.14 for FDG and 1.06 ± 0.14 for total ^{19}F (mean ± SE; $n = 7$). In contrast, the rate of formation of new FDM showed large decreases of up to 5-fold. In five of seven cases, low levels of FDM (30–90 nmol) could still be detected 48 h after the first FDG treatment, and in two of seven cases, the FDG group was detectable (38 and 43 nmol). This is consistent with the observations of Kanazawa *et al.* (3, 6), who reported that UDP-FDM persisted for at least 48 h in heart, muscle, and particularly ascites tumor cells. Where detectable (five of seven), the mean FDM concentration was 0.077 ± 0.023 mM (±SE), ~30% of the maximum amount eventually formed after the second injection of FDG.

Correlation between Tumor Response and FDG Metabolism Before and After 5FU Treatment. All RIF-1 tumors treated with 5FU responded by a decrease in volume that was clearly visible after 48 h. However, the extent of the response expressed either as the MXD or TV7 was variable. The MXD correlated strongly with TV7 ($r = 0.85$; $P = 0.017$), which suggested that both measurements were valid assessments of 5FU cytotoxicity.

Fig. 4, *a* and *b*, shows that prior to 5FU treatment, the four ^{19}F MRS parameters of total ^{19}F signal, FDG, FDM AUC, and FDM rate correlated positively with tumor response expressed as TV7, but this was only significant for the FDM AUC, $r = 0.81$ ($P = 0.028$; Fig. 4*b*). A similar pattern was seen if tumor response was expressed using MXD, although in all cases the correlation was weaker and did not reach significance for FDM. After 5FU treatment (Fig. 4, *c* and *d*), the change in AUC for FDG or ^{19}F signal showed no correlation with response but was stronger for FDM AUC and significant for the FDM rate when response was expressed as MXD, $r = 0.80$ ($P = 0.032$; Fig. 4*d*). When the four parameters were correlated with TV7, the same pattern was observed of FDM correlating most strongly with response: $r = 0.29$, 0.21, 0.34, and 0.63 for the AUCs of ^{19}F, FDG, FDM, and FDM rate, respectively.

Discussion

To our knowledge, this is the first demonstration that administration of FDG leads to uptake and metabolism by solid tumors that is detectable noninvasively by ^{19}F MRS *in vivo*. Furthermore, one of the metabolites formed, α-FDM and its conjugates, correlated with tumor response to 5FU treatment, whereas total ^{19}F signal or FDG and its conjugates did not correlate significantly. These observations demonstrate that FDG can undergo considerable metabolism in solid tumors and suggests that methods that only detect total label, *e.g.*, ^{18}FDG, would be less likely to predict tumor response.

Glucose Utilization by Tumors. The high glycolytic rates exhibited by solid tumors permit their detection *in situ*, because trace levels of radioactive FDG, ^{18}FDG, can be measured by the highly sensitive technique of PET (2). FDG enters the cells via the facilitative glucose carrier, is phosphorylated by a HK to FDG-6P, but then unlike glucose, is believed to undergo little further metabolism, so that ^{18}FDG becomes trapped (2). It is assumed that for a tumor to accumulate glucose, it must be viable, and thus a change in glucose accumulation would reflect a change in tumor viability or metabolic activity. This hypothesis is the rationale for the application of PET to detect changes in tumor glucose utilization soon after treatment, as an early predictor of tumor response. However, the approach has not always been successful, perhaps because of the variety of biochemical responses that can occur after therapy. For example, tumor blood flow may increase or decrease, and the immune response may also be unpredictable (2, 11). In addition, the method detects total label and relies upon a three-compartment model to obtain rates of glucose

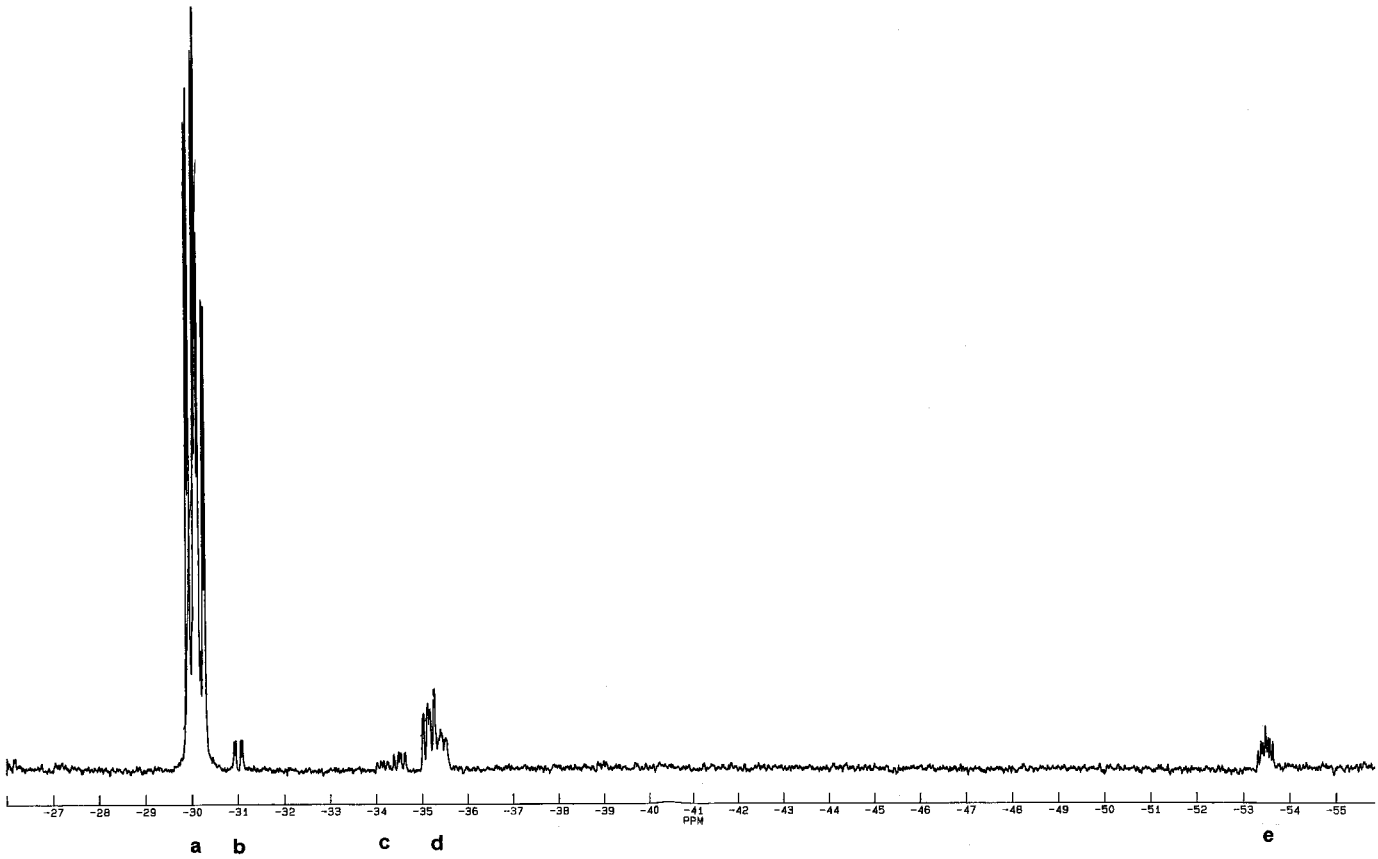

Fig. 3. ^{1}H-coupled ^{19}F MRS spectrum of a RIF-1 tumor extract made 2 h after FDG administration. Peaks are referenced to 5FU (0 ppm) as follows. *Group a:* β-and α-anomers of FDG-1P, FDG-1,6P_2, and FDG-6P. *Group b:* β- and α-anomers of NDP-FDG. *Group c:* α-anomers of FDM-1,6P_2 and 1P. *Group d:* α-anomers of FDM-6P, FDM, and NDP-FDM. *Group e:* β-anomers of FDM-6P, FDM, and NDP-FDM.

uptake and phosphorylation or dephosphorylation. In principle, a method that can distinguish the metabolites of FDG would improve modeling of glucose utilization.

^{19}F MRS of FDG. The first reported demonstration by ^{19}F MRS that FDG is metabolized beyond FDG-6P was in rat brain *in vivo* (12), and this was repeated in mouse ascites (4), heart, muscle, and liver (6), all *ex vivo*. Although the first metabolite of FDG, FDG-6P, cannot be resolved from FDG *in vivo*, the primary metabolites of the PPP (Fig. 1) could be detected in brain, heart, and particularly liver, 3 ppm downfield from FDG (6, 12). In extracts of mouse ascites, these PPP metabolites were identified only at very low levels (3). In contrast, the major metabolite in all organs, except liver, appeared to be α-FDM$\pm$P, leading eventually to UDP-FDM (Fig. 1). UDP-FDM persists for 12–48 h at near mM concentrations in ascites cells, and this permitted fluoroimaging *in vivo* (3). Formation of FDM-6P is likely to occur through epimerization of FDG-6P via the enzyme PGI, although this is not proven (5). PGI is widely distributed in the cytoplasmic compartment of the cell, measurable amounts exist in the serum, and erythrocytes, liver, muscle, bone, brain, and lung are rich in PGI (9). In fact, plasma levels of PGI are raised in metastatic cancer and can be used as an index of tumor growth or activity in the body (13).

It is conceivable that FDM is formed through isomerization of FDG, via GI in the tumor cell, plasma, or a major organ, followed by conversion to FDM-6P via HK and then to FDG$\pm$6P and UDP conjugates of FDM and FDG in the tumor (Fig. 1). In this case, inhibition of PGI would not prevent formation of FDM phosphates and UDP-FDM. The second metabolite in the PPP, 6PG, is a strong inhibitor of PGI, and high levels of 6PG are thought to be responsible for inhibition of glycolysis in RIF-1 cells after incubation of the cells with 6AN (Fig. 1; Ref. 14). We found that 6AN blocked formation of ^{19}F MRS detectable FDM$\pm$P but not formation of UDP-FDG, suggesting that at least in tumor cells, the major source of FDM formation is through the action of the enzyme PGI. Furthermore, FDM was not detectable in plasma, and the rate of formation of FDM in isolated RIF-1 cells was similar to that measured *in vivo*. All of which suggests that the FDM$\pm$P detected in tumors *in vivo* probably results entirely from conversion of FDG-6P to FDM-6P by PGI and not from FDM circulating in the plasma after FDG metabolism by other tissues. The rate of FDM formation occurs at ~1% of the rate of glucose consumption reported in rat breast xenograft tumors (15), presumably because the epimerization by PGI is relatively inefficient. For FDM formation to be a surrogate for HK activity, PGI activity would have to greatly exceed HK activity, and indeed we observed a relative ratio of 64:1. In contrast, brain, heart, and erythrocytes have relative ratios of 5, 9, and 17, respectively, but skeletal muscle, a tissue that has the capacity for high glycolytic rates, has a ratio of 117 (16). RIF-1 tumors are known to be very glycolytic (17), and thus the high PGI/HK may be indicative of strongly glycolytic cells.

Correlation of FDG Metabolism with Tumor Response. There was a significant correlation between the change in rate of FDM formation and response, a weaker correlation between the FDM AUC and response, and no correlation with FDG or total ^{19}F signal. Thus, 2 days after treatment, only the FDM signal could be used to predict the extent of tumor response to treatment. The calculation was, however, complicated by the presence in most cases of residual FDM (presumably mostly UDP-FDM) from the first FDG dose. This amount had to be measured first, so that the true amount of new FDM

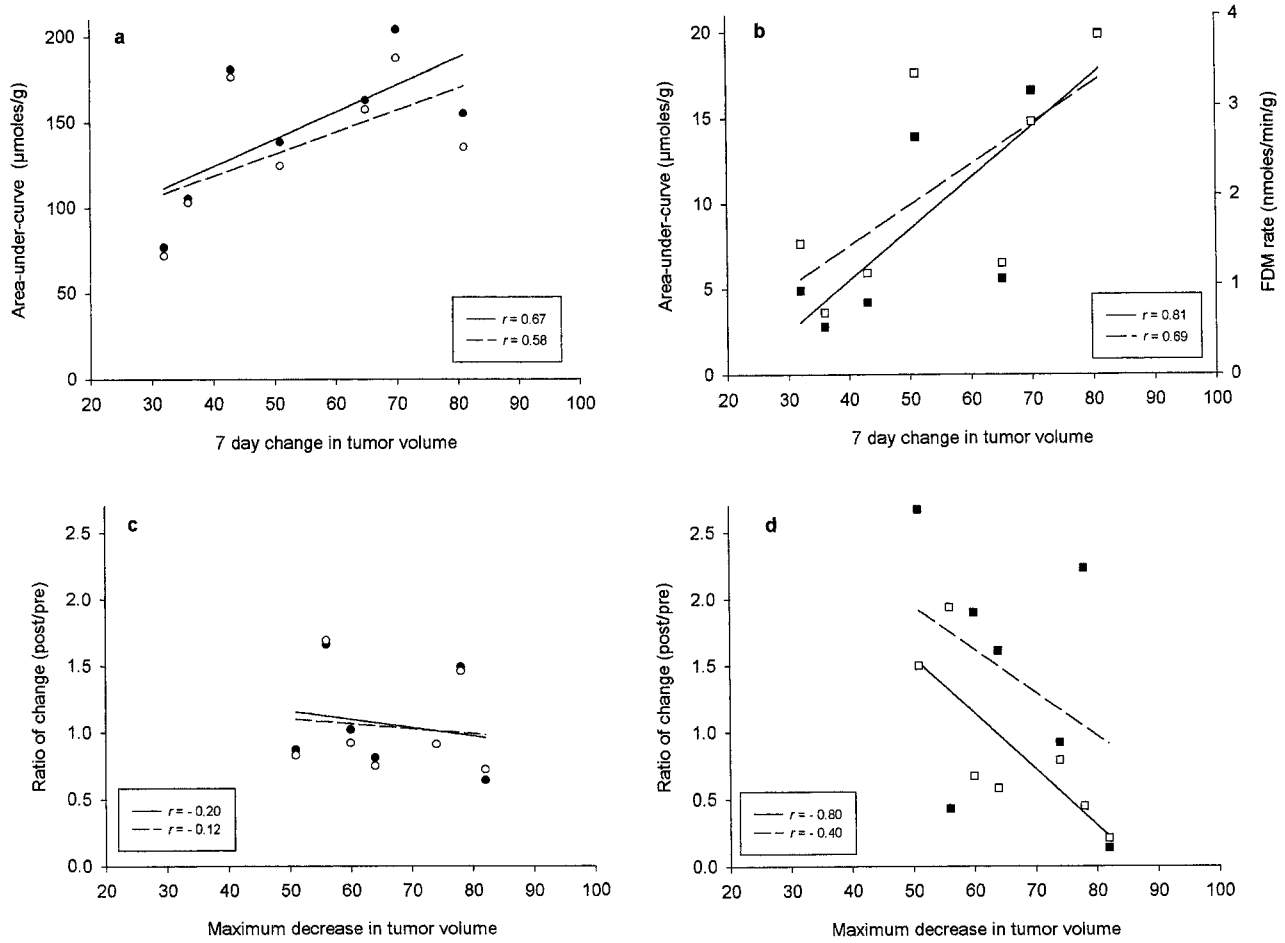

Fig. 4. Correlation of pretreatment FDG metabolism (*a* and *b*) and change in FDG metabolism after 5FU treatment (*c* and *d*) with tumor response to 5FU. *a*, AUCs for FDG, ○, and total ^{19}F signal, ●, $r = 0.58$, $P = 0.17$ and $r = 0.67$, $P = 0.10$, respectively. *b*, FDM AUC, ■, and rate of FDM formation, □, $r = 0.81$, $P = 0.028$ and $r = 0.69$ and $P = 0.085$, respectively. *c*, change in AUCs for FDG, ○, and total ^{19}F-signal, ●, $r = -0.20$, $P = 0.80$ and $r = -0.12$, $P = 0.68$, respectively. *d*, change in FDM AUC, ■, and rate of FDM formation, □, $r = -0.4$, $P = 0.37$ and $r = -0.80$, $P = 0.032$, respectively.

could be determined, otherwise the FDM would have been overestimated. It is also conceivable that these residual FDM metabolites could inhibit the activity of the enzymes PGI, PGM, and glucose-1-phosphate uridyltransferase and thus lead to underestimation of the amount of FDG-6P that was formed. Most of the 5FU administered would be metabolized to fluoro-uridine phosphates, including FUDP-glucose (8), and this might interfere with FDG metabolism in an unpredictable manner. Nevertheless, overall the results indicated that the tumors showing the largest change in tumor volume had a decrease in the rate of FDM formation (five of seven; Fig. 4*d*), implying a decrease in the rate of glucose phosphorylation and thus glycolysis. This is consistent with the report of Aboagye *et al.* (18), who showed that a similar dose of 5FU (160 mg/kg i.p.) induced a mean decrease in total lactate formation by RIF-1 tumors of 50–70%, 24–48 h after treatment. Thus, the response of RIF-1 tumors to 5FU probably involves a decrease in the rate of glycolysis, and this may be detected by ^{19}F MRS as a decrease in the rate of formation of FDM from FDG. In the model of Aboagye *et al.* (18), it was concluded that the decrease in tumor volume occurred through apoptotic cell death, and therefore, changes in tumor viability were attributable to changes in cell viability rather than changes in tumor blood flow.

Considering the potential complications of residual FDM and the effects of 5FU on FDG metabolism, it is also important that positive correlations were found between ^{19}F levels and tumor response prior to 5FU treatment (Fig. 4, *a* and *b*). This was strongest for FDM and was significant for the FDM AUC ($r = 0.81$; $P = 0.03$). Removal of glucose from the plasma and lactate formation have been found to be highly variable in rat xenograft models but were shown to be proportional to tumor blood flow and inversely proportional to tumor wet weight (15). In a hormone-responsive rat tumor model, deoxyglucose uptake postovariectomy correlated with the number of S-phase cells and tumor blood flow, but more strongly with the latter (11). These articles suggest that high glucose utilization may reflect both the ease with which a drug enters the tumor space as well as the number of cycling cells, important parameters determining tumor drug sensitivity. For 5FU sensitivity, FDG may reflect tumor blood flow, but metabolism to FDM may be a better indicator of cell viability.

Toxicity. About 30 years ago, experiments with deoxyfluoropyranoses focused on their potential as anti-cancer agents through their ability to inhibit glycolysis (19). Although high concentrations of ≥5 mM could inhibit growth *in vitro*, similar plasma concentrations had little effect on mouse tumors *in vivo*. The LD_{50} was reached at daily doses ≥1.5 mmol/kg (3, 19). In our experiments, mice received a single dose of 5FU plus two doses of FDG separated by 48 h, and there was no significant increase in animal or tumor toxicity compared with that measured in the model where animals received only 5FU (7). However, if FDG was administered 24 h after 5FU and therefore just 24 h after the first FDG dose, then two of three animals died. Otherwise, the dose we have used of 1.4 mmol/kg i.p. of FDG, which produced a plasma concentration of 1.6 mM, appears not to be significantly toxic. Furthermore, our unpublished observations suggest that a lower dose of 1 mmol/kg provides sufficient signal-to-noise ratio to

detect FDM in RIF-1 and other murine tumors of ~1 g, and much lower doses may be possible in rat tumors, which can be used at volumes of 5–10 g.

In conclusion, RIF-1 tumors are capable of forming considerable amounts of FDM from FDG, and this may be detected by ^{19}F MRS *in vivo*. The rate and/or amount of FDM formation, but not the total FDG or ^{19}F signal, correlated significantly with the response of the tumors to 5FU treatment. Considerations of the known biochemical response of RIF-1 tumors to 5FU suggest that decreases in the rate of formation of FDM reflect decreases in the rate of glycolysis in these tumors. We are currently aiming to determine whether: (*a*) FDM formation reflects HK activity; and (*b*) FDM formation can predict tumor response to other chemotherapeutic agents. If the latter is verified, then ^{19}F MRS of FDG metabolism may prove to be a novel means of predicting tumor response noninvasively, which would have useful clinical applications. Indeed, because human tumors at presentation tend to be quite large compared with animal tumors, this would permit lower FDG doses to be used of ~0.2 g/m^2, thus decreasing the likelihood of any toxicity.

Acknowledgments

We thank Jon Cobb of the Department Chemistry, Kings College, London, for the use of the 8.5T Bruker instrument.

References

1. Weber, G. Biochemical strategy of cancer cells and the design of chemotherapy. Cancer Res., *43:* 3466–3492, 1983.
2. Rigo, P., Paulus, P., Kaschten, B. J., Hustinx, R., Bury, T,. Jerusalem, G., Benoit, T., and Foidart-Willems, J. Oncological applications of positron emission tomography with fluorine-18 fluorodeoxyglucose. Eur. J. Nucl. Med., *23:* 1641–1674, 1996.
3. Kanazawa, Y., Umayahara, K., Shimmura, T., and Yamashita, T. ^{19}F NMR of 2-deoxy-2-fluoro-D-glucose for tumor diagnosis in mice. An NDP-bound hexose analog as a new NMR target for imaging. NMR Biomed., *10:* 35–41, 1997.
4. Kojima, M., Kuribayashi, S., Kanazawa, Y., Haradahira, T., Maehara, Y., and Endo, H. Metabolic pathway of 2-deoxy-2-fluoro-D-glucose and 2-deoxy-2-fluoro-D-mannose in mice bearing sarcoma-180 studied by 19F-MRS. Chem. Pharm. Bull., *36:* 1191–1197, 1988.
5. Pouremad, R., and Wyrwicz, A. M. Cerebral metabolism of fluorodeoxyglucose measured with ^{19}F NMR spectroscopy. NMR Biomed., *4:* 161–166, 1991.
6. Kanazawa, Y., Yamane, H., Shinohara, S., Kuribayashi, S., Momozono, Y., Yamato, M., Kojima, M., and Masuda, K. 2-Deoxy-2-fluoro-D-glucose as a functional probe for NMR: the unique metabolism beyond its 6-phosphate. J. Neurochem., *66:* 2113–2120, 1996.
7. McSheehy, P. M. J., Robinson S. P., Ojugo, A. S. E., Aboagye, E. O., Cannell, M., Leach, M. O., Judson, I. R., and Griffiths, J. R. Carbogen breathing increases 5-fluorouracil uptake and cytotoxicity in hypoxic RIF-1 tumours: a magnetic resonance study *in vivo*. Cancer Res., *58:* 1185–1194, 1998.
8. McSheehy, P. M. J., Prior, M. J. W., and Griffiths, J. R. Prediction of 5-fluorouracil cytotoxicity towards the Walker carcinosarcoma using peak integrals of fluoronucleotides measured by MRS *in vivo*. Br. J. Cancer, *60:* 303–309, 1989.
9. Bergmeyer, H. U. Methods of Enzymatic Analysis, Ed. 2, Vol. 1, pp. 121–501, and Vol. 4, p. 1112. New York: Verlag Chemie, Weinheim, Academic Press, 1974.
10. Braunschweiger, P. G. Effect of cyclophosphamide on the pathophysiology of RIF-1 solid tumors. Cancer Res., *48:* 4206–4210, 1988.
11. Carnochan, P., and Brooks, R. Radiolabelled 5′-iodo-2′-deoxyuridine: a promising alternative to [^{18}F]-2-fluoro-2-deoxy-D-glucose for PET studies of early response to anticancer treatment. Nucl. Med. Biol., *26:* 667–672, 1999.
12. Nakada, T., Kwee, I. L., and Conboy, C. B. Non-invasive *in vivo* demonstration of 2-fluoro-2-deoxy-D-glucose metabolism beyond the hexokinase reaction in rat brain by ^{19}F nuclear magnetic resonance spectroscopy. J. Neurochem., *46:* 198–201, 1986.
13. Bodansky, O. Serum phosphohexose isomerase in cancer; as index of tumor growth in metastatic carcinoma of prostate. Cancer (Phila.), *8:* 1087–1114, 1955.
14. Street, J. C., Mahmood, U., Ballon, D., Alfieri, A. A., and Koutcher, J. A. ^{13}C and ^{31}P NMR investigation of effect of 6-aminonicotinamide on metabolism of RIF-1 tumor cells *in vitro*. J. Biol. Chem., *271:* 4113–4119, 1996.
15. Kallinowski, F., Vaupel, P., Runkel, S., Berg, G., Fortmeyer, H. P., Baessler, K. H., Wagner, K., Mueller-Klieser, W., and Walenta, S. Glucose uptake, lactate release, ketone body turnover, metabolic micromilieu and pH distributions in human breast cancer xenografts in nude rats. Cancer Res., *48:* 7264–7272, 1988.
16. Newsholme, E. A., and Start, C. Chapter 3. *In:* Regulation in Metabolism, p. 99. New York: John Wiley and Sons, 1973.
17. Bhujwalla, Z. M., Constantinidis, I., Chatham, J. C., Wehrle, J. P., and Glickson, J. D. Energy metabolism, pH changes and lactate production in RIF-1 tumors following intratumoral injection of glucose. Int. J. Radiat. Oncol. Biol. Phys., *22:* 95–101, 1992.
18. Aboagye, E. O., Bhujwalla, Z. M., Shungu, D. C., and Glickson, J. D. Detection of tumor response to chemotherapy by ^{1}H nuclear magnetic resonance spectroscopy: effect of 5-fluorouracil on lactate levels in radiation-induced fibrosarcoma-1 tumors. Cancer Res., *58:* 1063–1067, 1998.
19. Bessell, E. M., Courtenay, V. D., Foster, A. B., Jones, M., and Westwood, J. H. Some *in vivo* and *in vitro* antitumour effects of the deoxyfluoro-D-gluco-pyranoses. Eur. J. Cancer, *9:* 463–470, 1973.